Structural Studies of Poly(*p*-phenyleneamine) and Its Oxidation

E. T. Kang,* K. G. Neoh, T. C. Tan, and S. H. Khor

Department of Chemical Engineering, National University of Singapore, Kent Ridge, Singapore 0511

K. L. Tan

Department of Physics, National University of Singapore, Kent Ridge, Singapore 0511

Received August 22, 1989; Revised Manuscript Received November 28, 1989

ABSTRACT: The structural changes associated with the chemical oxidation of poly(*p*-phenyleneamine) or "leucoemeraldine" (PLM) were determined quantitatively by X-ray photoelectron spectroscopy (XPS) and qualitatively by infrared (IR) absorption spectroscopy and thermogravimetric analysis (TGA). XPS and IR data showed that some of the amine repeating units of PLM were oxidized slowly by oxygen to the imine structure. Treatment of PLM with 1 M HCl involved a gradual oxidation of the polymer to give rise to a partially protonated emeraldine (PEM). Oxidation of PLM by chlorine resulted in a nitrogenonium ion structure analogous to that arising from the protonation of imine nitrogen in PEM by HCl. However, a substantial amount of the halogen dopant was incorporated into the polymer as covalent chlorine even at low chlorine loading. Oxidative "doping" of PLM by organic electron acceptors such as tetrachloro-*o*-benzoquinone (*o*-chloranil) and tetrabromo-*o*-benzoquinone (*o*-bromanil) involved first the oxidation of the amine nitrogen and also the formation of the imine structure through hydrogen transfer from the pristine amine nitrogen to the acceptor. The so-produced imine nitrogen was in turn doped by the acceptor. XPS data of the PLM–halobenzoquinone complexes indicated that the nitrogenonium cations of the polymer were balanced by the halogen and the oxygen or benzoquinone anions.

Introduction

The discovery of the exceptional electrical properties of polyacetylene[1] has spurred a great deal of research work in the area of electroactive polymers in recent years.[2] Of particular interest is the century-old[3] aniline family of polymers. The polymers are basically poly(*p*-phenyleneamine–imines) in which the oxidation state can be varied from the fully reduced poly(*p*-phenyleneamine) or "leucoemeraldine" to the fully oxidized poly(*p*-phenyleneimine) or "pernigraniline". The 50% oxidized poly(*p*-phenyleneamine–imine) has been termed "emeraldine base".[4] The electrical conductivity of the polymer could be increased from ca. 10^{-11} to over 1 S/cm either by varying the number of electrons per repeat unit through oxidative doping or by the addition of protons associated with individual nitrogen sites.[4–9]

The chemical structures of emeraldine (PEM) and its salt complexes have been studied extensively by electron spectroscopy for chemical analysis (ESCA) or X-ray photoelectron spectroscopy (XPS),[10–14] infrared (IR) absorption spectroscopy,[15–18] and NMR[19–21] as well as by the study of model compounds.[22,23] A number of studies have also been devoted to the fully reduced leucoemeraldine (PLM) and its oxidized complexes.[8,9,18,20] This report deals with a detailed analytical study on the intrinsic structure of PLM and the structural changes associated with the oxidative chemical "doping" of PLM by some proton-free electron acceptors, using XPS, IR absorption, and thermogravimetric analysis (TGA). Structural changes associated with the protonation of PLM by HCl are also explored and compared with the published data.

Our recent studies[24,25] have demonstrated that the proportions of quinonoid imine, benzenoid amine, and positively charged nitrogen in polyaniline can be determined quantitatively and unambiguously from the properly deconvoluted N1s XPS core-level spectrum. For example, the N1s core-level spectrum of PEM base can be fitted with two Gaussian peaks of about equal size with binding energies (BE) of 399.3 ± 0.1 and 398.1 ± 0.1 eV. The peaks have been assigned to the amine and imine nitrogen, respectively. The assignment is consistent with the fact that PLM, which is comprised entirely of reduced amine repeating units,[20] exhibits only a single N1s environment at 399.3 eV. Furthermore, "doping" of PEM by protonic acid results in the reduction or disappearance of the imine peak component and the appearance of a high-BE tail above 401 eV. The latter is attributable to the positively charged nitrogen. This again is consistent with the fact that protonation of PEM base occurs preferentially at the imine repeating units.[4,8] The contribution of chemically different nitrogen atoms to the broad N1s spectrum has been suggested in an early study.[11] It has also been reported recently that the composition of the neutral nitrogen, the radical cation, and the cation in electrochemically oxidized or acid-protonated PLM can be determined from the XPS N1s and valence band spectra.[9] However, the proportions of imine and amine repeating units corresponding to a particular oxidation state of the polymer were not quantitatively resolved.

Experimental Section

Polymer Samples. Emeraldine hydrochloride was prepared by the oxidative polymerization of aniline by ammonium persulfate in 1 M HCl according to the method reported in the literature.[4] Thus, 0.05 mol of aniline was dissolved in 800 mL of 1 M HCl. The solution was kept at 0–5 °C under a nitrogen atmosphere. A prechilled solution of 0.05 mol of ammonium persulfate in 200 mL of 1 M HCl was added slowly with vigorous stirring. The reaction mixture was agitated continuously for another 5 h. The precipitate was subsequently filtered and collected. It was converted to emeraldine base (PEM) by treatment with excess 0.5 M aqueous NH_4OH and dried by pumping under reduced pressure. The leucoemeraldine (PLM) was obtained by treatment of PEM with excess phenylhydrazine according to the method of Green and Woodhead.[3] Oxidative doping of PLM was carried out by dispersion of the fine polymer powder in acetonitrile solution of the acceptor under a nitrogen atmosphere and with vigorous agitation. The complexes were dried by pumping under reduced pressure. The electron

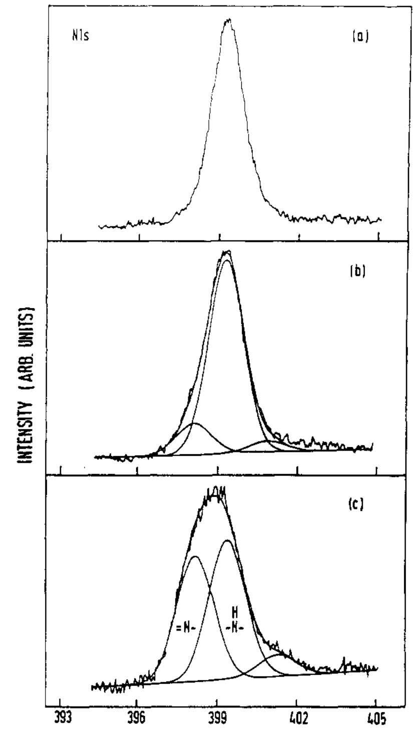

Figure 1. N1s XPS core-level spectra of (a) freshly prepared PLM, (b) PLM after exposure to dry air for 2 months, and (c) PEM base.

acceptors used included chlorine and organic electron acceptors such as tetrachloro-*o*-benzoquinone (*o*-chloranil) and tetrabromo-*o*-benzoquinone (*o*-bromanil). The halobenzoquinone acceptors were obtained from Aldrich Chemical Co. and were recrystallized from chloroform solution. "Protonation" of PLM was carried out by treating the polymer with 1 M HCl as in the case of protonation of PEM base by HCl.[4]

Polymer Characterization. The electrical conductivities of the complexes were measured by using the standard collinear four-probe and two-probe techniques on compressed pellets. The infrared (IR) absorption spectra measurements were carried out on a Perkin-Elmer Model 682 spectrophotometer with the polymer samples dispersed in KBr. Thermogravimetric analysis (TGA) was carried out with a Netzsch simultaneous TG–DTA apparatus, Model STA 409, at a heating rate of 10 °C/min in nitrogen. XPS measurements were carried out on a VG ESCALAB MkII spectrometer with a Mg Kα X-ray source (1253.6-eV photons). The polymer samples in powder form were mounted on the standard sample studs by means of double-sided adhesive tape. The X-ray power supply was run at 12 kV and 10 mA. Pressure in the analysis chamber during the scans was maintained at or lower than 10^{-8} mbar. All core-level spectra were referenced to the C1s neutral carbon peak at 284.6 eV. The peak width (full width at half-maximum or fwhm) was maintained constant for all components in a particular spectrum during deconvolution. The peak area ratios for various elements were corrected by experimentally determined instrumental sensitivity factors and may be subjected to ±10% error. In most cases, the surface composition determined by XPS agreed fairly well with the bulk composition.

Results and Discussion

Structure and Properties of Leucoemeraldine. We first explore the intrinsic stability of leucoemeraldine. Figure 1a shows the N1s XPS core-level spectrum of a freshly prepared PLM sample. As expected, the sample exhibits only a single nitrogen environment at a binding energy (BE) of 399.3 eV, which is characteristic of the amine structure.[24,25] Figure 1b shows the spectrum of the sample after exposure to dry air for 2 months. The spectrum is skewed somewhat toward the low-BE side.

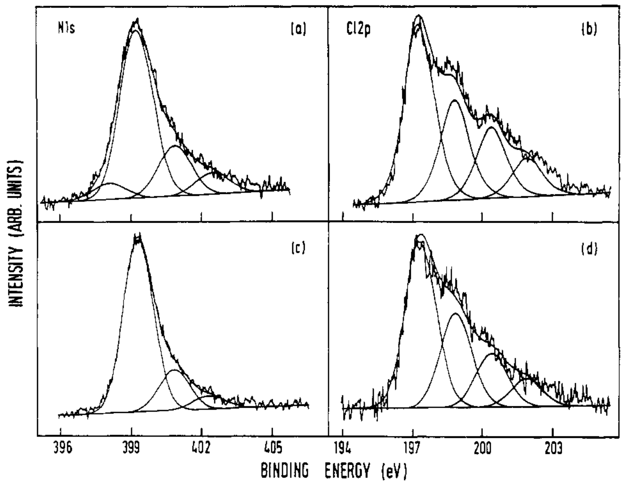

Figure 2. N1s and Cl2p XPS core-level spectra of (a, b) PEM/HCl complex, and (c, d) freshly prepared PLM/HCl complex.

A new peak component with BE characteristic of the imine repeating units (398.1 eV) is resolvable. Thus, the present XPS data give further support to the earlier suggestion that some of the amine units are oxidized to the imine units in the presence of oxygen.[8] However, we wish to emphasize that the oxidation of PLM by air or oxygen proceeds only very slowly. The process is further retarded in the presence of an inert atmosphere. The presence of a small high-BE tail probably arises from some surface oxidation of the sample. For comparison purposes, the curve-fitted N1s core-level spectrum of a PEM base, which consists of about equal amounts of imine and amine repeating units,[4] is shown in Figure 1c. The respective Gaussian components at 398.1 and 399.3 eV are attributable to the imine and amine nitrogens.[24,25]

Protonation of PEM by acids represents a new concept in conducting polymers and is by far the most commonly practiced method of obtaining highly conductive polyaniline complexes. Thus, an attempt was made to compare the acid protonation of PLM with that of PEM. Figure 2 shows the N1s and Cl2p XPS core-level spectra for the PEM and PLM base after treatment with 1 M HCl. The final Cl/N ratios for the PEM/HCl and PLM/HCl complexes, as determined from corrected Cl2p and N1s spectral area ratios, are 0.44 and 0.36, respectively. The N1s core-level spectrum reveals the presence of only residual imine structure in the PEM/HCl complex, as indicated by the presence of a small peak component at 398.1 eV.[24,25] This is consistent with the fact that protonation of PEM occurs preferentially at the imine repeating unit.[4,24] Furthermore, the presence of a single peak at 399.3 eV together with a high-BE tail in the N1s spectrum of the freshly prepared PLM/HCl complex suggests that protonation occurs at the amine units in PLM. Protonation of the amine nitrogens in PLM has been suggested in an earlier study.[9] The presence of a similar high-BE tail above 401 eV in both of the present complexes is consistent with the formation of positively charged nitrogens.[10,12,24] The high-BE tail in the present PLM/HCl complex, however, differs somewhat from that of the PLM treated with 2 M hydrofluoroboric acid.[9] In this latter complex, a prominent peak component was observed at 402.4 eV and has been attributed to the protonated amine nitrogen. It should be noted that the protonated amine structure, at least in the case of the present PLM/HCl complex, exists only as a metastable state and is gradually transformed into a structure similar to that of partially protonated PEM. This is indicated by the gradual appearance of a low-BE imine component in the

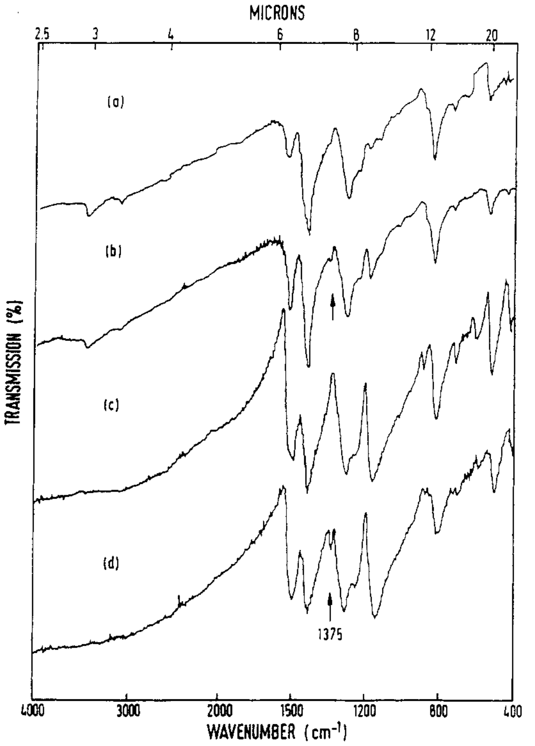

Figure 3. IR absorption spectrum of (a) fresh PLM, (b) PLM exposed to dry air for 2 months, (c) fresh PLM/HCl complex, and (d) PLM/HCl complex after 2 months.

N1s spectrum of the PLM/HCl complex and is further supported by the corresponding change in the IR absorption spectrum (see below). The electrical conductivity of the PLM/HCl complex is on the order of 10^{-2} S/cm, which is 2 orders of magnitude lower than that of the PEM/HCl complex.[4] The Cl2p XPS core-level spectra of both complexes show striking similarity. Deconvolution gives rise to Cl2p$_{1/2}$ and Cl2p$_{3/2}$ components at BE positions corresponding to those for covalent and ionic chlorine species. Thus, as much as 25% of the chlorine can become covalently bonded to the polymer in both complexes and the degree of protonation should not be determined from the total Cl/N ratio. A possible explanation for the presence of covalent chlorine is the formation of C–Cl bonds on the aromatic rings. Chlorination of the aniline rings has been suggested during the oxidation of PLM by Cl_2.[8] The Cl2p$_{3/2}$ BE corresponding to the respective ionic and covalent chlorine occurred at ca. 197.1 and 200.3 eV in both complexes. Thus, no significant shift in the Cl2p BE is observed between the protonation of imine nitrogen and that of amine nitrogens. This observation differs from that of the electrochemically prepared polyaniline complexes, in which a BE difference of 1.4 eV has been suggested for the ionic chlorines resulting from protonation of imine and amine nitrogens.[13]

Traces a and b of Figure 3 show the respective IR absorption spectra of the freshly prepared and aged PLM base. Earlier studies[17,18] have suggested that the modes at ca. 1500 and 1600 cm^{-1} are associated with the aromatic ring stretching. Tang et al.[16] have associated the peak at ca. 1500 cm^{-1} with the benzenoid (B) ring and the absorption at 1600 cm^{-1} with the quinonoid (Q) ring. When applied to the IR spectrum of PLM, which exhibits a very low 1600 cm^{-1}/1500 cm^{-1} intensity ratio, this assignment is supportive of a structure rich in B units. The increase in the 1600 cm^{-1}/1500 cm^{-1} intensity ratio upon aging of PLM is thus consistent with the oxidation of amine units to imine units, as is also suggested by the XPS data. Another informative peak in the IR spectra of polyaniline is the weak C–N stretching absorption in QBQ units[16] at ca. 1375 cm^{-1}. PLM does not absorb at this frequency. On the other hand, PEM base, which consists of about equal amounts of B and Q units, absorbs at 1375 cm^{-1}.[16] However, upon acid protonation of PEM base, the Q units are believed to be converted to B units by the proton-induced spin-unpairing mechanism, and the absorption at 1375 cm^{-1} disappears.[15,16] These observations suggest that the weak absorption band at 1375 cm^{-1} can be qualitatively linked to the existence of Q and B units in the polymer. This is further supported by the fact that the appearance of a small amount of imine structure in aged PLM (Figure 1b) is accompanied by the appearance of a weak 1375-cm^{-1} absorption in the IR spectrum of Figure 3b. Figure 3c shows the IR absorption spectrum of a freshly prepared PLM/HCl sample. The intense broad band at ca. 1150 cm^{-1} is characteristic of the doped or protonated imine or amine structure.[16] The absence of the 1375-cm^{-1} absorption and the relatively low 1600 cm^{-1}/1500 cm^{-1} intensity ratio indicate that the freshly prepared PLM/HCl complex contains predominantly B units and protonation by HCl occurs at the amine nitrogen sites.

Interesting changes in the IR spectrum of the PLM/HCl complex are observed upon aging of the sample. Figure 3d shows the IR absorption spectrum of a PLM/HCl complex 2 months after protonation. A new absorption band at 1375 cm^{-1} has appeared, and the intensities of the 1600- and 1500-cm^{-1} bands have become almost equal. The IR absorption spectrum now resembles that of a partially protonated PEM/HCl complex, consistent with the XPS results. We wish to point out that this transformation in the IR absorption has virtually completed after 1 week, with the color of the complex changed from green to black. Furthermore, deprotonation of this aged PLM/HCl complex with 0.5 M NaOH gives rise to an IR absorption spectrum not unlike that of the PEM base. The N1s XPS core-level spectrum of this deprotonated sample further confirms the appearance of a large proportion of the imine component at the BE position of 398.1 eV, similar to that observed in the PEM base. Thus, protonation of PLM by HCl must have also resulted in a subsequent oxidation of the amine units to the imine units, probably through the removal of protons as in the case of oxidation by oxygen. Some of the newly formed imine nitrogens are simultaneously protonated by the existing HCl.

The thermal behaviors of the PLM base, PEM base, and their salt complexes are compared in Figure 4. TGA scans suggest that both cases exhibit remarkable similarity in thermal stability, with the major weight loss occurring only at temperatures above 400 °C. The initial weight loss at temperatures below 100 °C observed in the PEM base has been attributed to the loss of residual water retained by the polymer during preparation.[26] The thermal stability of both bases is substantially reduced upon salt complex formation and will be discussed in the next section.

Oxidation by Chlorine. Earlier studies[7,8] suggested that the oxidation of PLM by halogens proceeded according to the scheme shown in Figure 5. Figure 6 shows the N1s and Cl2p XPS core-level spectra for three PLM/Cl_2 samples at low, moderate, and high chlorine concentrations. Each chlorine spectrum can again be curve-fitted with Cl2p$_{1/2}$ and Cl2p$_{3/2}$ components at BE positions corresponding to those for covalent and ionic chlorine species. The Cl2p$_{3/2}$ BE corresponding to these two species are at ca. 200.4 and 197.0 eV, respectively. Thus, a sub-

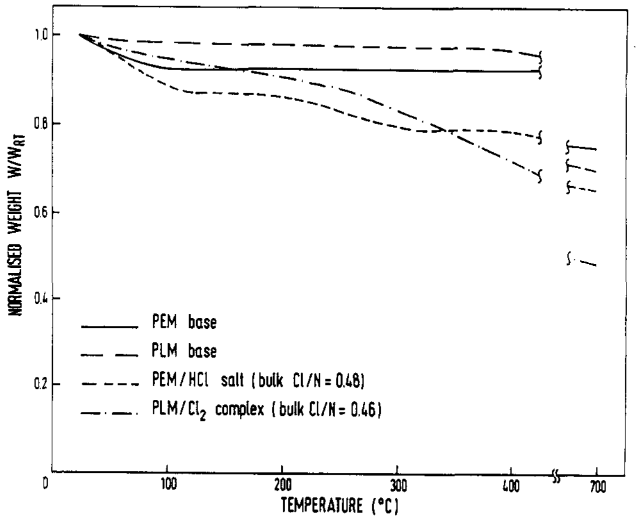

Figure 4. TGA scans of PLM, PEM, PEM/HCl complex, and PLM/Cl_2 complex.

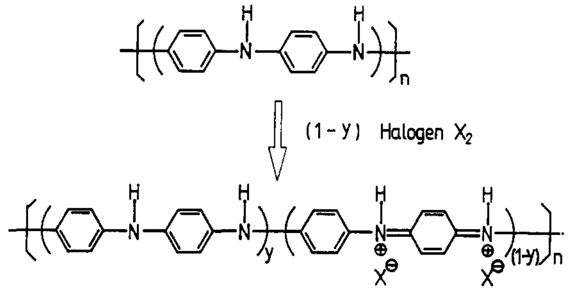

Figure 5. Schematic representation of the oxidative doping of PLM by halogens.

stantial amount of chlorine is covalently bonded to the polymer even at low chlorine concentrations. At high chlorine loading, the acceptor exists largely as covalent chlorine. The N1s spectrum reveals the presence of a predominantly amine structure, as indicated by the major peak component at 399.3 eV. The high-BE tail above 401 eV is again characteristic of positively charged nitrogen.[10,12,24]

Table I summarizes the surface stoichiometries, the chemical states of the acceptor, and the oxidation states of the polymer for some of the PLM/Cl_2 complexes studied. For most of the complexes, the composition, as indicated by the Cl/N ratio, at the surface agrees fairly well with that of the bulk obtained from elemental analysis. The data in Table I readily suggest that there exists an optimal chlorine concentration at which the proportions of chloride anion, positively charged nitrogen, and the electrical conductivity reach a maximum. In all samples studied, a close balance between the number of chloride anions and the number of positively charged nitrogens is observed. The presence of localized unit positive charge on the nitrogen is consistent with the concept of the nitrogenonium ion polymer of MacDiarmid et al.[4] and has been favored by Munro et al.[12] The slight excess of positively charged nitrogen observed in the present complexes is probably attributable to the presence of surface oxidation products and contaminants, as suggested by the presence of a weak O1s core-level signal. The presence of surface oxidation has also been observed for the electrochemically prepared polyanilines.[13]

The maximum electrical conductivity observed in the present PLM/Cl_2 complexes is about 1 order of magnitude higher than that reported in the literature.[8] The presence of increasing proportions of covalently bonded chlorine upon increasing the halogen loading readily suggests that the electrical conductivity of the complexes cannot be easily correlated with the total acceptor level. Furthermore, the degree of oxidation of the complexes should not be determined from overall halogen balance alone.

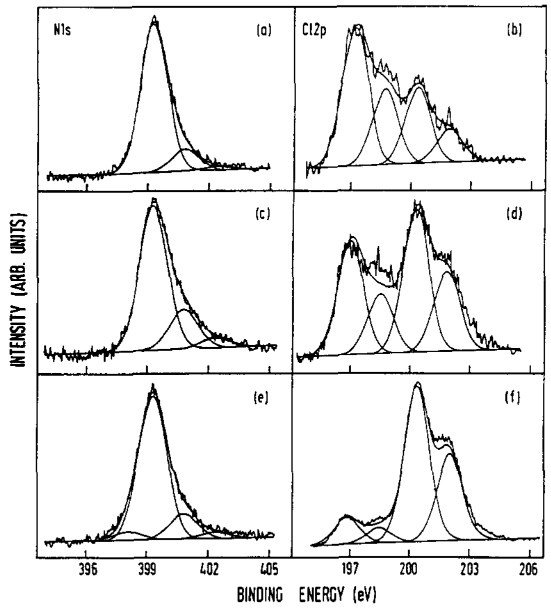

Figure 6. N1s and Cl2p XPS core-level spectra for three PLM/Cl_2 complexes with surface Cl/N ratios of (a, b) 0.14, (c, d) 0.39, and (e, f) 0.94.

Finally, Figure 5 suggests that oxidation of PLM by chlorine gives rise to a nitrogenonium ion structure analogous to that of the protonated imine nitrogen in PEM. Thus "deprotonation" of PLM/Cl_2 complexes should also result in the appearance of the imine structure. Figure 7 shows the corresponding N1s and Cl2p core-level spectra for the three complexes of Figure 6 after treatment with 0.5 M NaOH. Thus base treatment has indeed resulted in the appearance of the imine structure at 398.1 eV and the complete removal of the chloride anion. Furthermore, as much as 30% of the covalently bonded chlorine in each sample is also removed during the NaOH treatment. This latter phenomenon suggests that covalent chlorine formation does not arise entirely from ring substitution. For substituted anilines such as 2-chloroaniline, 3-chloroaniline, and 4-chloroaniline polymerized in the presence of 1 M H_2SO_4 and ammonium persulfate, elemental analysis and XPS data show that treatment of the polymer complexes with 0.5 M NaOH does not cause a significant change in the Cl/N ratio.

The IR absorption spectra of a PLM/Cl_2 complex before and after deprotonation by NaOH are shown in Figure 8. The IR spectrum of the PLM/Cl_2 complex shows a close resemblance to that of the PEM/HCl complex.[16] Furthermore, Figure 8b suggests that NaOH treatment of the PLM/Cl_2 complex gives rise to a structure similar to that of the PEM base rather than that of the PLM base. The appearance of the weak absorption band at 1375 cm^{-1} again suggests the presence of quinonoid rings. Thus the IR absorption spectra give further support to the XPS data, and the interaction of chlorine with PLM results in a nitrogenonium ion structure analogous to that of the HCl-protonated imine nitrogen in PEM.

Careful inspection of the N1s spectra of Figure 7 further suggests that the proportion of imine nitrogen arising from the "deprotonation" process in each sample appears to be somewhat higher than the Cl^-/N ratio. This may serve to indicate that the basic structure and oxidation state of the polymer must have been altered by

Table I
XPS Results and Stoichiometries of the Various Leucoemeraldine/Chlorine Complexes

sample no.	bulk Cl/N	surface stoichiometries[a] Cl/N	-Cl/N	Cl^-/N	proportion of =N-[b]	-NH-	N^+	conductivity σ, S/cm
1	0.12	0.14	0.04	0.10	0.0	0.85	0.15	8×10^{-3}
2	0.20	0.25	0.09	0.16	0.0	0.79	0.21	6×10^{-2}
3	0.46	0.39	0.21	0.18	0.0	0.75	0.25	1.0
4	0.54	0.67	0.48	0.19	0.02	0.76	0.22	8×10^{-1}
5	0.68	0.94	0.79	0.15	0.03	0.78	0.18	4×10^{-1}
6	0.86	1.10	1.00	0.10	0.02	0.83	0.15	7×10^{-2}

[a] Based on the corrected chlorine/nitrogen core-level spectral area ratios. [b] Neutral imine structure.

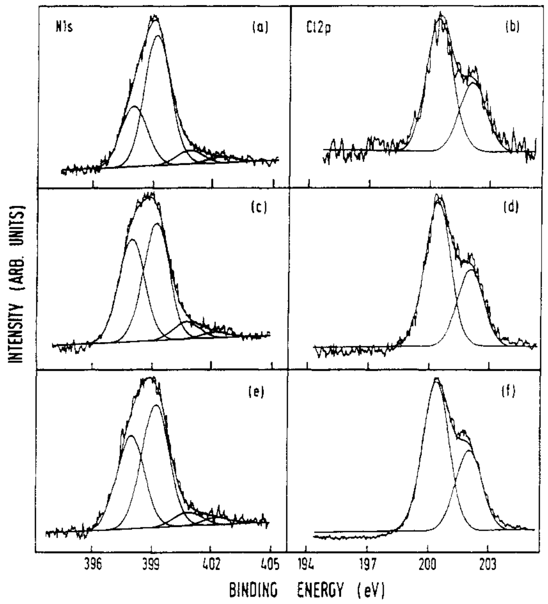

Figure 7. N1s and Cl2p XPS core-level spectra for the three PLM/Cl_2 complexes shown in Figure 6 after treatment with 0.5 M NaOH.

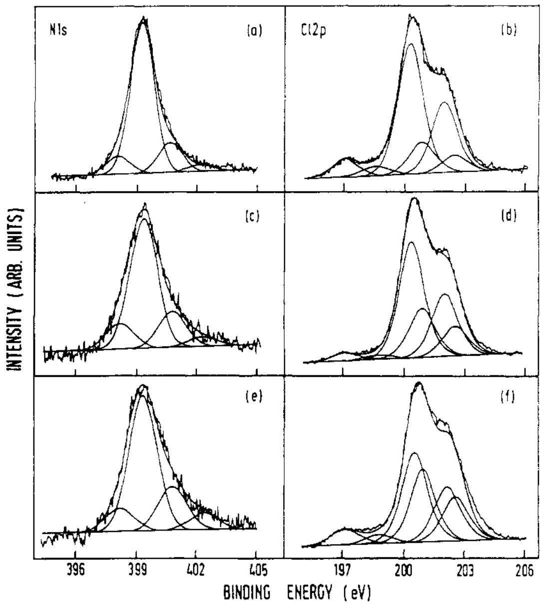

Figure 9. N1s and Cl2p XPS core-level spectra for three PLM/*o*-chloranil complexes with surface *o*-chloranil/monomer ratios of (a, b) 0.14, (c, d) 0.30, and (e, f) 0.44.

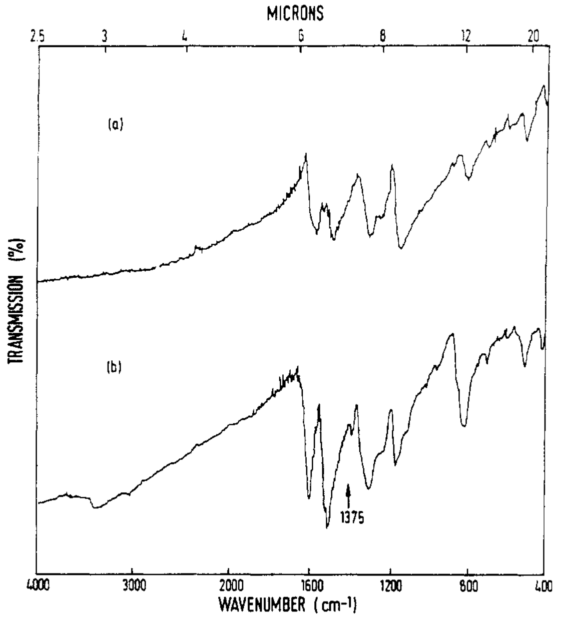

Figure 8. IR absorption spectra of (a) PLM/Cl_2 complex (bulk Cl/N = 0.46) and (b) PLM/Cl_2 complex after NaOH treatment.

the covalent chlorine formation. This is further supported by the difference in weight loss behavior between the PLM/Cl_2 and PEM/HCl complexes shown in Figure 4, with the latter retaining a substantially higher weight when heated to high temperature. Furthermore, although the complexes have comparable bulk Cl/N ratios, comparison of the Cl2p core-level spectra in Figures 2b and 6d suggests that the PEM/HCl complex contains a substantially high fraction of ionic chloride. This may help to account for the higher initial weight loss observed in the PEM/HCl complex, during which PEM/HCl decomposes by the loss of protonic acid.[26]

Oxidative "Doping" by Organic Acceptors. Interesting changes in the structure and oxidation states of the polymer are observed during the oxidative "doping" of PLM by the halobenzoquinones *o*-chloranil and *o*-bromanil. Figure 9 shows the curve-fitted N1s and Cl2p core-level spectra for three PLM/*o*-chloranil complexes. The N1s and Br3d core-level spectra for three PLM/*o*-bromanil complexes are shown in Figure 10. The detailed chemical states of the acceptor and the oxidation states of the polymer for the respective PLM/*o*-chloranil and PLM/*o*-bromanil complexes studied are summarized in Tables II and III.

The N1s core-level spectra in Figures 9 and 10 show a gradual decrease in the amine structure and the simultaneous appearance of both the imine structure at ca. 398.1 eV and the positively charged nitrogen at BE >401 eV upon progressive "doping" of PLM by the organic acceptors. However, at high acceptor loading, the amount of imine structure decreases and is accompanied by a continuing increase in the amounts of positively charged nitrogen and the halogen anions. These suggest that two distinct processes must have been involved in the doping of PLM by the organic acceptors. The presence of halogen anion, as suggested by the occurrence of a low-BE component in the Cl2p and Br3d core-level spectra,[27] readily indicates that some cleavage of the C–Cl and C–Br bonds of the acceptors must have occurred. Furthermore, Fig-

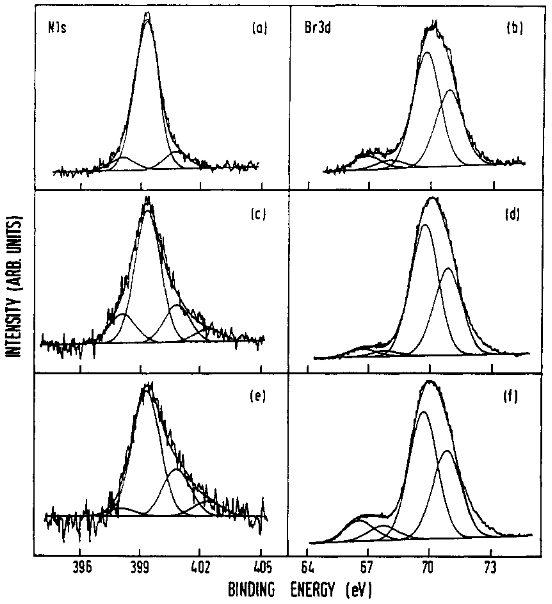

Figure 10. N1s and Br3d XPS core-level spectra for three PLM/*o*-bromanil complexes with surface *o*-bromanil/monomer ratios of (a, b) 0.04, (c, d) 0.25, and (e, f) 0.40.

ure 11 shows the O1s XPS core-level spectrum for a typical PLM/*o*-chloranil complex. The O1s envelope suggests the presence of three different oxygen environments. A similar O1s line shape has also been observed for the PLM/*o*-bromanil complex. The center peak component with a BE of ca. 532 eV is attributable to the carbonyl oxygen of the acceptor. The low-BE component that is shifted by ca. −1.5 eV from the center peak is attributable to the oxygen anion, such as the benzoquinone or semibenzoquinone anion.[27,28] On the other hand, a positive BE shift of 1.5 eV is consistent with the formation of the structure of the type C–O–, such as the hydrobenzoquinone structure. The formation of the benzoquinone anions and hydrobenzoquinone structure is consistent with a substantial reduction in the C=O stretching vibration[29] at ca. 1700 cm^{-1} in the infrared absorption spectra of the present complexes (see Figure 14). The formation of these structures has also been widely observed in molecular donor–acceptor interactions. For example, in the charge-transfer interaction between *N*,*N*-dimethylaniline and *p*-chloranil, a detailed mechanism involving electron transfer to yield the aniline radical cation and the halobenzoquinone radical anion has been proposed.[30] The latter transforms readily into the hydroquinone anion structure via a hydrogen atom transfer reaction from the former. The involvement of both halogen and oxygen anions in the present complexes is further supported by the fact that the amount of positively charged nitrogen in Tables II and III is closely balanced by the sum of the halogen and oxygen anions. Finally, it is appropriate to point out that the presence of surface oxidation products and contaminants, which has also been reported for the electrochemically prepared polyanilines,[13] may have also contributed to some extent to the present O1s spectrum.

Based on the present XPS results and the proposed mechanism of charge-transfer interaction in similar donor–acceptor systems,[28,30] a plausible mechanism for the interaction between PLM and the halobenzoquinone is depicted in Figure 12. Thus the initial stage of oxidative doping must involve predominantly the oxidation of amine nitrogen since it is the only site available. The cleavage of the halogen from the acceptor molecules and the formation of halobenzoquinone radical anion would probably result in the subsequent abstraction or transfer of an amine hydrogen to satisfy the valency requirement of the halobenzoquinone molecules. This is consistent with the simultaneous appearance of the imine nitrogen and the positively charged nitrogen. The somewhat higher proportion of the latter at low acceptor level is probably attributable to the surface oxidation products[13] and/or the doping of some of the newly formed imine nitrogen by the acceptor (see below). At high acceptor loading, the disappearnce of the imine structure and the substantial increase in the amounts of positively charged nitrogen and the halogen anions are consistent with the doping of the imine repeating units by the acceptor. This additional step proposed for the doping mechanism can then help to explain the striking increase in the electrical conductivity of the PLM/*o*-bromanil complex at high acceptor level (sample 5, Table III).

The existence of two distinct doping processes is further supported by the number of chlorine environments resolvable from the Cl2p core-level spectrum of the PLM/*o*-chloranil complex. At low acceptor level, Figure 9 suggests the presence of a major covalent chlorine environment with a $Cl2p_{3/2}$ BE of 200.3 eV. This BE is separated by 3.2 eV from the ionic components at ca. 197.1 eV. A second covalent chlorine environment with a slightly higher $Cl2p_{3/2}$ BE of ca. 200.7 eV (and thus an ionic–covalent separation of 3.6 eV) is required to complete the simulation. The intensity of this higher BE component increases with increasing acceptor loading. The lower BE component suggests the presence of covalently bonded chlorine in a more electron-rich environment such as the hydrobenzoquinone anion structure shown in Figure 12e. The predominance of this structure at low acceptor levels is consistent with the presence of a relatively high proportion of the oxygen or benzoquinone anions and the corresponding proportion of the imine structure. As the acceptor loading increases, neutral halobenzoquinone structures and halobenzoquinone structures resulting from the charge-transfer interaction with the imine nitrogens become more significant, and thus one observes an increase in the higher BE covalent component. For example, charge-transfer interaction between excess *o*-chloranil and imine nitrogen of PEM gives rise to a Cl2p spectrum with a BE separation of ca. 3.6 eV between ionic and covalent chlorine component (see below). In the case of *o*-bromanil complex, the different covalent environment cannot be resolved from the Br3d core-level spectrum, probably due to the lower electronegativity of bromine. However, a slight increase in the line width of the Br3d high-BE component is observed at high acceptor loading.

The proposed mechanism for the interaction between imine nitrogen and the halobenzoquinones is similar to that proposed for the charge-transfer interaction between *p*-chloranil and the nitrogen atom of molecular pyridine (=N– structure) to account for the presence of positively charged pyridinium nitrogen and the chloride and benzoquinone anions.[28] The preferential interaction of the halobenzoquinones with the imine units upon their formation in the present complexes is further supported by the following experimental evidence. In the charge-transfer interaction involving PEM, which consists of equal numbers of imine and amine nitrogens, and *o*-chloranil, the XPS results suggest the presence of chloride and benzoquinone anions. The structural change of PEM upon complex formation is readily revealed by the N1s core-level spectrum of the complexes, as shown in Figure 13 for three PEM/*o*-chloranil complexes at low, moderate, and high acceptor loading. The gradual decrease in the proportion of the imine structure at 398.1 eV and the

Table II
XPS Results and Stoichiometries of the Leucoemeraldine/*o*-Chloranil Complexes

			ratio[c] of		proportion of			conductivity
sample no.	bulk *o*-chloranil/N ratio[a]	surface *o*-chloranil/N ratio[b]	Cl^-/N	$-O^-/N$	-N=[d]	-NH-	N^+	σ, S/cm
1	0.09	0.14	0.06	0.10	0.09	0.73	0.18	3×10^{-5}
2	0.12	0.23	0.05	0.11	0.13	0.66	0.21	2×10^{-4}
3	0.32	0.30	0.07	0.14	0.13	0.64	0.23	3×10^{-2}
4	0.31	0.44	0.18	0.13	0.10	0.63	0.27	0.1
5	0.56	0.60	0.22	0.13	0.10	0.59	0.31	0.3

[a] Determined gravimetrically. [b] Based on the corrected total halogen/nitrogen area ratio. [c] Based on the anion peak component/total nitrogen area ratio. [d] Neutral imine structure.

Table III
XPS Results and Stoichiometries of the Leucoemeraldine/*o*-Bromanil Complexes

			ratio[c] of		proportion of			conductivity
sample no.	bulk *o*-bromanil/N ratio[a]	surface *o*-bromanil/N ratio[b]	Br^-/N	$-O^-/N$	-N=[d]	-NH-	N^+	σ, S/cm
1	0.04	0.04	0.02	0.04	0.07	0.83	0.10	3×10^{-5}
2	0.10	0.11	0.04	0.06	0.11	0.74	0.15	4×10^{-5}
3	0.20	0.24	0.07	0.11	0.11	0.72	0.17	4×10^{-5}
4	0.30	0.25	0.08	0.12	0.14	0.63	0.23	3×10^{-5}
5	0.50	0.40	0.17	0.13	0.04	0.64	0.32	2×10^{-2}

[a-d] See footnotes of Table II.

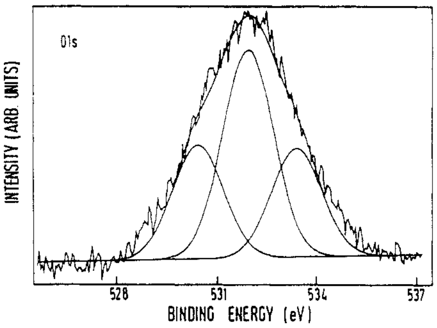

Figure 11. O1s XPS core-level spectrum of a PLM/*o*-chloranil complex at a surface *o*-chloranil/monomer ratio of 0.30.

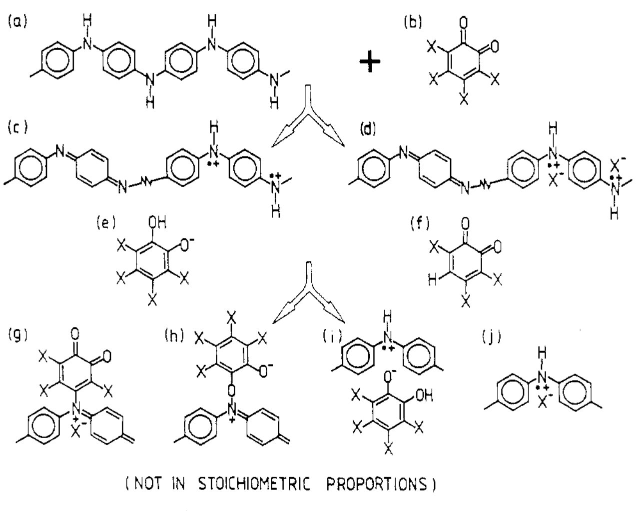

Figure 12. Possible mechanisms of interaction between PLM and the halobenzoquinones.

corresponding increase in the amount of positively charged nitrogen readily indicate that the charge-transfer interactions in PEM/*o*-chloranil complex occur preferentially at the imine repeating units. More importantly, the Cl2p core-level spectrum suggests the presence of only one covalent chlorine environment with a $Cl2p_{3/2}$ BE component at ca. 3.6 eV above that of the ionic chlorine. Similar changes in the N1s line shape and the formation of halogen and benzoquinone anions are also observed during the charge-transfer interactions between PEM and *o*-bromanil. All these are consistent with the formation of the structures proposed in Figure 12g,h.

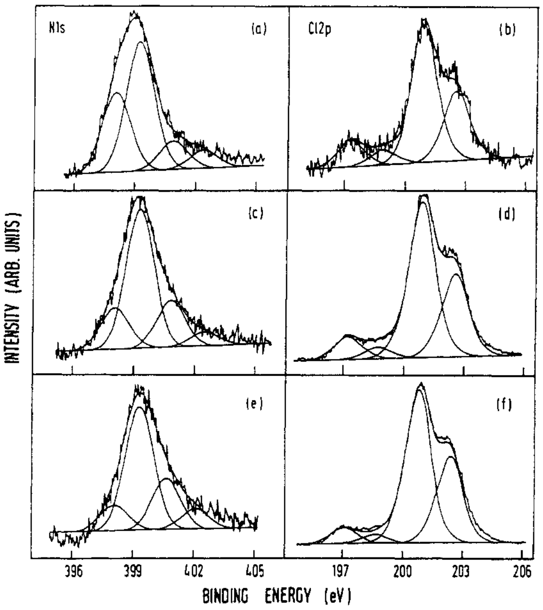

Figure 13. N1s and Cl2p XPS core-level spectra for three PEM/*o*-chloranil complexes with surface *o*-chloranil/monomer ratios of (a, b) 0.12, (c, d) 0.45, (e, f) 0.71.

The proposed mechanism of the charge-transfer interactions between PLM and halobenzoquinone acceptor is further supported by the IR absorption data. Figure 14 shows the IR absorption spectra of two PLM/*o*-bromanil samples at relatively low and high acceptor level and a PLM/*o*-chloranil sample at moderate acceptor level. Upon incorporation of a small amount of halobenzoquinone, the absorption band at 1375 cm^{-1}, which is absent in the original PLM base, begins to appear. The 1375-cm^{-1} band, however, disappears upon increasing the acceptor loading (Figure 14b). Since this band is associated with the existence of quinonoid units, its appearance at low acceptor level corresponds to the oxidation of the amine nitrogen and the formation of quinonoid imine structure by the acceptor, as shown in Figure 12. Its disappearance upon increasing the acceptor loading is consistent with the "doping" of the newly formed imine nitrogens by the acceptor. With the exception of highly "doped" samples, the absorption bands due to the organic acceptors are not clearly visible in most of the present PLM/

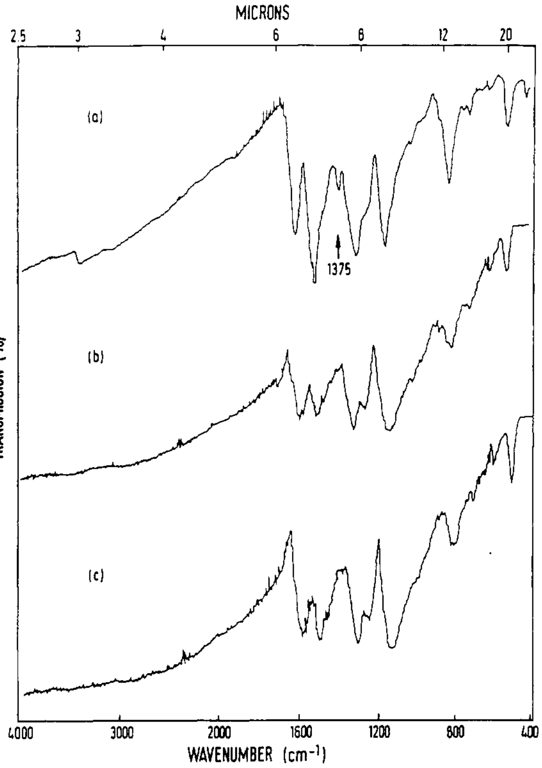

Figure 14. IR absorption spectra of PLM/halobenzoquinone complexes with o-bromanil/monomer ratios of (a) 0.04 and (b) 0.50 and (c) with o-chloranil/monomer ratio of 0.23.

halobenzoquinone complexes. The absence of anionic absorption bands has also been reported in other conjugated polymer complexes involving inorganic[31] and organic acceptors.[32] In fact, for organic complexes, the deviation of the IR absorption spectrum of the complex from the sum of the spectra of the two components has been used to differentiate between weak charge-transfer complexes and the products of electron-transfer reaction.[33]

Finally, Figure 15 shows the thermogravimetric scans of two PLM/o-bromanil complexes and a PLM/o-chloranil complex. In comparison with the pristine PLM, the onset temperature for the major weight loss is substantially lower for all of the organic acceptor complexes. Furthermore, the thermal stability appears to decrease with increasing acceptor concentration. At high acceptor loading, the onset temperature of major weight loss in both PLM/o-chloranil and PLM/o-bromanil complexes coincides roughly with the decomposition temperature of the respective organic acceptor. Thus the thermal decomposition behavior of the present complexes is probably associated with the removal or decomposition of the acceptor incorporated. This is further supported by the fact that the weight of the complexes retained at high temperature decreases with increasing acceptor concentration.

Conclusion

The structural changes associated with the oxidative doping of poly(p-phenyleneamine) or leucoemeraldine (PLM) by oxygen, hydrochloric acid, chlorine, o-chloranil, and o-bromanil were studied by X-ray photoelectron spectroscopy (XPS), infrared (IR) spectroscopy, and thermogravimetric analysis (TGA). In all cases, some of the amine units of PLM were oxidized to the imine units by the acceptors. In the case of PLM/HCl and PLM/Cl_2 complexes, a significant amount of chlorine was incorporated as covalent chlorine, and the structure of both complexes is analogous to that of HCl-protonated emeraldine (PEM) base. Interaction of PLM with the halobenzoquinones involved first the oxidative "doping" of the amine units and then the "doping" of the imine units produced in the first step. The formation of chloride and benzoquinone anions suggested that the oxidation of PLM by the organic acceptors had proceeded further than the pure formation of molecular charge-transfer complexes.

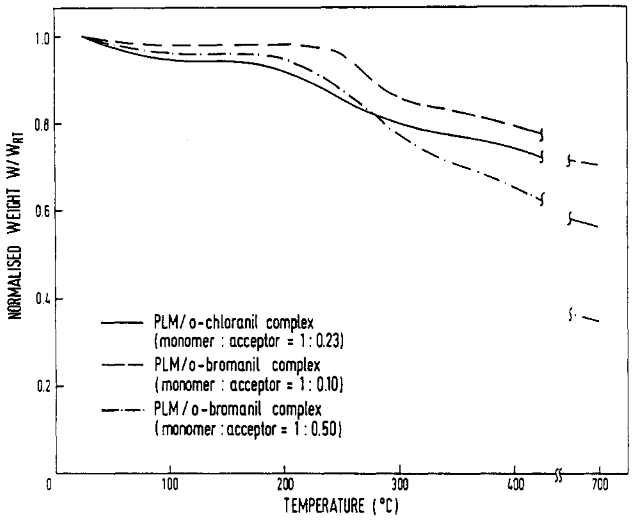

Figure 15. TGA scans of some PLM/halobenzoquinone complexes in nitrogen.

References and Notes

(1) Chiang, C. K.; Fincher, C. R., Jr.; Park, Y. W.; Heeger, A. J.; Shirakawa, H.; Louis, E. J.; Gau, S. C.; MacDiarmid, A. G. *Phys. Rev. Lett.* **1977**, *39*, 1098.
(2) See, for example: Skotheim, T., Ed. *Handbook of Conducting Polymers*; Marcel Dekker: New York, 1986; Vols. I, II.
(3) Green, A. G.; Woodhead, A. E. *J. Chem. Soc.* **1910**, 2388.
(4) Chiang, J. C.; MacDiarmid, A. G. *Synth. Met.* **1986**, *13*, 193. MacDiarmid, A. G.; Chiang, J. C.; Richter, A. F.; Epstein, A. J. *Synth. Met.* **1987**, *18*, 285.
(5) MacDiarmid, A. G.; Chiang, J. C.; Halpern, M.; Huang, W. S.; Mu, S. L.; Somasiri, N. L. D.; Wu, W.; Yaniger, S. I. *Mol. Cryst. Liq. Cryst.* **1985**, *121*, 173.
(6) Diaz, A. F.; Logan, J. A. *J. Electroanal. Chem. Interfacial Electrochem.* **1980**, *111*, 111.
(7) Leclerc, M.; Guay, J.; Dao, L. H. *Macromolecules* **1989**, *22*, 649.
(8) Ray, A.; Asturias, G. E.; Kershner, D. L.; Richter, A. F.; MacDiarmid, A. G.; Epstein, A. J. *Synth. Met.* **1989**, *29*, E141.
(9) Nakajima, T.; Harada, M.; Osawa, R.; Kawagoe, T.; Furukawa, Y.; Harada, I. *Macromolecules* **1989**, *22*, 2644.
(10) Salaneck, W. R.; Lundstrom, I.; Hjertberg, T.; Duke, C. B.; Conwell, E.; Paton, A.; MacDiarmid, A. G.; Somasiri, N. L. D.; Huang, W. S.; Richter, A. F. *Synth. Met.* **1987**, *18*, 291.
(11) Snauwaert, P.; Lazzaroni, R.; Riga, J.; Verbist, J. J. *Synth. Met.* **1987**, *18*, 335.
(12) Munro, H. S.; Parker, D.; Eaves, J. G. *Springer Ser. Solid-State Sci.* **1987**, *76*, 257.
(13) Mirrezaei, S. R.; Munro, H. S.; Parker, D. *Synth. Met.* **1988**, *26*, 169.
(14) Hagiwara, T.; Demura, T.; Iwata, K. *Synth. Met.* **1987**, *18*, 317.
(15) Ohsaka, T.; Ohnuki, Y.; Oyama, N.; Katagiri, G.; Kamisako, K. *J. Electroanal. Chem. Interfacial Electrochem.* **1984**, *161*, 399.
(16) Tang, J.; Jing, X.; Wang, B.; Wang, F. *Synth. Met.* **1988**, *24*, 231.
(17) Kim, Y. H.; Foster, C.; Chiang, J.; Heeger, A. J. *Synth. Met.* **1988**, *25*, 49.
(18) Cao, Y.; Li, S.; Xue, Z.; Guo, D. *Synth. Met.* **1986**, *16*, 305.
(19) Hjertberg, T.; Salaneck, W. R.; Lundstrom, I.; Somasiri, N. L. D.; MacDiarmid, A. G. *J. Polym. Sci., Polym. Lett. Ed.* **1985**, *23*, 503.
(20) Menardo, G.; Nechtchein, M.; Rousseau, A.; Travers, J. P.; Hany, P. *Synth. Met.* **1988**, *25*, 311.
(21) Kaplan, S.; Conwell, E. M.; Richter, A. F.; MacDiarmid, A. G. *Synth. Met.* **1989**, *29*, E235.

2926 *Macromolecules* **1990,** *23,* 2926–2934

(22) Hjertberg, T.; Sandberg, M.; Wennerstrom, O.; Lagerstedt, I. *Synth. Met.* **1987**, *21*, 31.
(23) Baughman, R. H.; Wolf, J. F.; Eckhardt, H.; Shacklette, L. W. *Synth. Met.* **1988**, *25*, 121.
(24) Tan, K. L.; Tan, B. T. G.; Kang, E. T.; Neoh, K. G. *Phys. Rev. B* **198.**, *39*, 8070.
(25) Kang, E. T.; Neoh, K. G.; Khor, S. H.; Tan, K. L.; Tan, B. T. G. *J. Chem. Soc., Chem. Commun.* **1989**, 696.
(26) Neoh, K. G.; Kang, E. T.; Khor, S. H.; Tan, K. L. *Polym. Degrad. Stab.* **1990**, *27*, 107.
(27) Kang, E. T.; Ti, H. C.; Neoh, K. G. *Polym. J.* **1988**, *20*, 845.
(28) Ng, K. T.; Hercules, D. M. *J. Am. Chem. Soc.* **1975**, *97*, 4168.
(29) Matsunaga, Y. J. *J. Chem. Phys.* **1964**, *41*, 6.
(30) Foster, R. *Organic Charge Transfer Complexes*; Academic Press: New York, 1969; 313 and references therein.
(31) Street, G. B.; Clark, T. C.; Krounbi, M.; Kanazawa, K. K.; Lee, V.; Pfluger, P.; Scott, J. C.; Weiser, G. *Mol. Cryst. Liq. Cryst.* **1982**, *83*, 253.
(32) Kang, E. T.; Neoh, K. G.; Tan, T. C.; Ong, Y. K. *J. Polym. Sci., Polym. Chem. Ed.* **1987**, *25*, 2143.
(33) Foster, R. *Organic Charge Transfer Complexes*; Academic Press: New York, 1969; Chapter 4.

Registry No. O_2, 7782-44-7; HCl, 7647-01-0; polyaniline (homopolymer), 25233-30-1; polyaniline (SRU), 32036-19-4; chlorine, 7782-50-5; *o*-chloranil, 2435-53-2; *o*-bromanil, 2435-54-3.

On the Mechanism of Craze Fibril Breakdown in Glassy Polymers

Larry L. Berger

E. I. du Pont de Nemours and Company, Inc., Central Research and Development Department, Experimental Station, Wilmington, Delaware 19898

Received August 3, 1989; Revised Manuscript Received December 15, 1989

ABSTRACT: Optical and transmission electron microscopy were used to investigate the mechanism of craze fibril growth and breakdown in a series of neat glassy polymers of poly(methyl methacrylate) (PMMA), poly(α-methylstyrene) (PαMS), and polystyrene (PS), as well as in fully compatible blends of poly(2,6-dimethyl-1,4-phenylene oxide) (PPO) and PS, all at a homologous $T_g - T = 75$ °C. The neat polymers were examined over a broad range of molecular weight M, and the PPO–PS system was studied as a function of the weight fraction of PPO (ϕ) in the blend. During a slow strain rate test, in which ~40 independent film squares were simultaneously monitored, the median tensile strains at which crazing, ϵ_c, and craze fibril breakdown, ϵ_b, occurred in each polymer were determined. For the neat polymers, with $M < M_c$ (where M_c is the critical molecular weight for entanglement effects on the zero-shear rate viscosity) no stable craze formation was observed (i.e., $\epsilon_b - \epsilon_c \approx 0$); for $M \approx (2\text{–}20)M_c$, $\epsilon_b - \epsilon_c$ increased strongly with M and at $M > 20M_c$, $\epsilon_b - \epsilon_c$ increased only weakly with increasing M. For the PPO–PS blends, ϵ_c was found to be roughly constant for $0.5 < \phi < 0.68$ whereas $\epsilon_b - \epsilon_c$ increased markedly at values of $\phi \geq 0.64$. In all cases, craze fibril breakdown was traced to the formation of a small pear-shaped void at the craze/bulk interface. The morphology and statistics of the craze breakdowns were combined with a detailed description of the craze microstructural parameters (i.e., the craze fibril diameter and craze fibril spacing) to advance a molecular model of craze breakdown. At these strain rates, craze breakdown is believed to occur by two events: (1) random chain scission to form the surfaces of the craze fibrils and (2) stress-mediated chain disentanglement, of a group of surviving strands, *at the craze/bulk interface*. The predictions of this model are in satisfactory agreement with the empirically determined molecular weight (or ϕ) dependence of ($\epsilon_b - \epsilon_c$).

Introduction

It is now well established that brittle fracture in many glassy polymers can be traced to the formation and subsequent breakdown of small fibrillated regions of stress-induced plastic deformation, crazes.[1-9] Consequently, the importance of crazing in controlling the macroscopic postyield mechanical properties of polymers remains an area of keen interest.[10] In particular, recent studies examining the role of molecular entanglements and the polymer network on craze growth have shed new light on the mechanism of craze fibril formation and the factors that govern the scale of fibrillation.[10-15] In contrast, however, our understanding of craze fibril breakdown is quite poor.

Generally it has been recognized that the process of craze growth gives rise to two unique regions within the craze:[1-4,9,16-18] (1) the craze/bulk interfaces, a thin (ca. 10–25-nm) strain-softened polymer layer in which craze fibrillation (and hence craze widening) takes place and (2) the craze midrib, a thin (ca. 50–100-nm-wide) polymer layer lying in the center of the craze, which forms immediately behind the advancing craze tip. It should be emphasized that an important distinction exists between these two regions. Namely, the relative position of the craze midrib does not change as the craze widens. On the other hand, as the craze boundaries advance by drawing fresh polymer from this interface, it continuously generates a new locally strain-softened region, concomitantly leaving behind the now strain-hardened craze fibrils. Thus, unlike the craze midrib, the immediate location of the craze boundaries is a function of the plastic strain. While these two regions can be readily distinguished by microscopic techniques, there is poor agreement as to the site of the early stages of craze breakdown.

Previous studies involving calculations of the stress field at the crack tip,[19-21] optical interferometry measurements of the advance of the craze tip in precracked samples,[22-24] morphological examinations of fracture surfaces,[2,16,18,25] and acoustic emission analysis have proposed,[26] from indirect measurements or theory, a microscopic mechanism of craze fibril breakdown. Recently,

0024-9297/90/2223-2926$02.50/0